Romanian Reports in Physics, Vol. 68, No. 2, P. 648–657, 2016

DIELECTRIC PROPERTIES OF COMPOSITES CONTAINING SILICONE RUBBER AND MULTIWALL CARBON NANOTUBES DECORATED WITH GOLD

A. PANTAZI[1], S. PALADE[1], C. BERBECARU[1,4], M. VECA[2], A. DINESCU[2], V. ŞCHIOPU[2], O. OPREA[3], D. DRAGOMAN[1],

[1] Faculty of Physics, University of Bucharest, P.O. Box MG-11, 077125 Bucharest, Romania
E-mails: apazaida@yahoo.com; busuioc_stefania@yahoo.com; berbecaru2ciceron@yahoo.com; danieladragoman@yahoo.com
[2] National Institute for Research and Development in Microtechnologies
126A Erou Iancu Nicolae St., 077190 Bucharest, Romania
E-mails: monica.veca@imt.ro; adrian.dinescu@imt.ro; veronica.schiopu@imt.ro
[3] Faculty of Applied Chemistry and Materials Science, Politehnica University Bucharest, 1–7 Polizu St., 011061 Bucharest, Romania, E-mail: ovidiu73@yahoo.com
[4] Romanian Materials Science-Crystal Growth Society, 077125 Bucharest, Romania

Received July 17, 2014

Abstract. The dielectric permittivity and losses of composites containing silicon rubber and multiwall carbon nanotubes decorated with gold were measured on wide temperature and frequency ranges. The permittivity decreases with increasing temperatures, increases with increasing nanotube mass concentration, and has weak frequency dependence. The losses depend non-uniformly on temperature and frequency.

Key words: silicon rubber, carbon nanotubes, composite materials, dielectric properties.

1. INTRODUCTION

Silicone rubber (SR), also known as polydimethylsiloxane, is formed from inorganic silicon-oxygen polymer chains that act as a backbone on which organic methyl groups are attached and rotate freely. The interest in SR is motivated by its better heat resistance, chemical stability, and electrical insulation compared to organic rubber polymers with carbon-based backbones [1]. Being an elastomer with good mechanical properties over large temperature ranges, SR is generally used as sealant. For other applications, SR is usually filled with micro or nanoparticles. For instance, when filled with micro and nano alumina, SR can act as a flexible microwave substrate due to its low dielectric constant [2], while carbon nanotube (CNT)-SR composites show improved electrical, thermal and mechanical properties [3] imparted by the CNT filler [4]. The fabrication methods and applications of CNT-polymer composites are reviewed in [5].

On the other hand, even the exceptional properties of CNTs could be enhanced by functionalization. For instance, CNTs decorated with metal oxide nanoparticles are very sensitive dopamine biosensors [6], ozone can be detected with CNTs decorated with palladium [7], CNTs decorated with metal nanoparticles are known to enhance Raman scattering [8], whereas Au-decorated CNTs are excellent gas sensors and biosensors [9]. Moreover, polymer composites containing multiwall CNTs (MWCNTs) decorated with Ag nanoparticles could be fabricated as conductive, flexible and stretchable films by the hot-rolling technique [10].

This paper is dedicated to the study of the dielectric behavior of composites containing red SR (RSR) and MWCNTs decorated with Au nanoparticles. Several samples with different Au-MWCNT mass content have been prepared and their dielectric constant has been measured over wide temperature and frequency ranges. The dielectric properties of the composites are found to depend on the mass concentration of Au-MWCNT, which is to be expected due to the interfacial Maxwell-Wagner polarization mechanism [11], but the general temperature and frequency behavior in RSR and in Au-MWCNT-RSR composites is similar. The investigations show that the permittivity can be controllably enhanced by increasing the Au-MWCNT mass content, but the losses are practically unaffected by this parameter. Moreover, the composites show almost reproducible values of permittivity and losses in wide heating-cooling cycles, which could make them suitable as dielectrics for equipments working in extreme temperature conditions.

2. PREPARATION AND CHARACTERIZATION OF Au-MWCNT-RSR COMPOSITES

The L-4060 type high-purity unfunctionalized MWCNTs purchased from Shenzhen Nanotechnologies Co. Ltd. China, with lengths and diameters between 5–15 μm and 40–60 nm, respectively, were first decorated with gold nanoparticles following the method described in [12] with slight modifications. In a typical experiment the as-received MWCNT were refluxed in nitric acid (70 %) for 6 hours and subsequently washed with deionized water until the filtrate reached a neutral pH. Thereafter, dried MWCNT were mechanically mixed with gold (III) acetate and heated to 200°C for 4 hours to obtain the Au-MWCNT. SEM images of the pristine and decorated MWCNTS are given in Fig. 1.

As can be seen from these images, the MWCNTs are not separated but form bundles/aggregates both before and after functionalization with Au nanoparticles having diameters around 8–9 nm. The tendency of CNTs to aggregate is well documented in literature, [13].

The Au-MWCNT-RSR composites were prepared by mechanically mixing the MWCNTs decorated with Au with RSR gasket sealant from the Den Braven Company. Composites with different Au-MWCNT mass concentrations were obtained by precisely weighing the two components of the mixture with a Sartorius

CPA225D-OCE analytical balance. Then, the as obtained composites were placed between two rectangular and parallel fresh polished copper plates, rinsed in benzene, and deposited in air for at least 10 days at room temperature to allow the completion of the curing process and mass stabilization. Composites containing RSR and unfunctionalized MWCNT from the same provider (MWCNT-RSR composites) were also prepared.

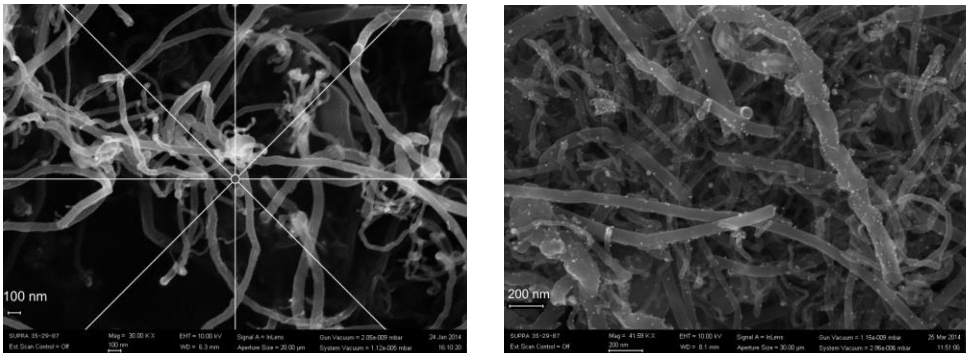

(a) (b)

Fig. 1 – SEM photo of (a) pristine MWCNTs and (b) MWCNTs decorated with Au nanoparticles.

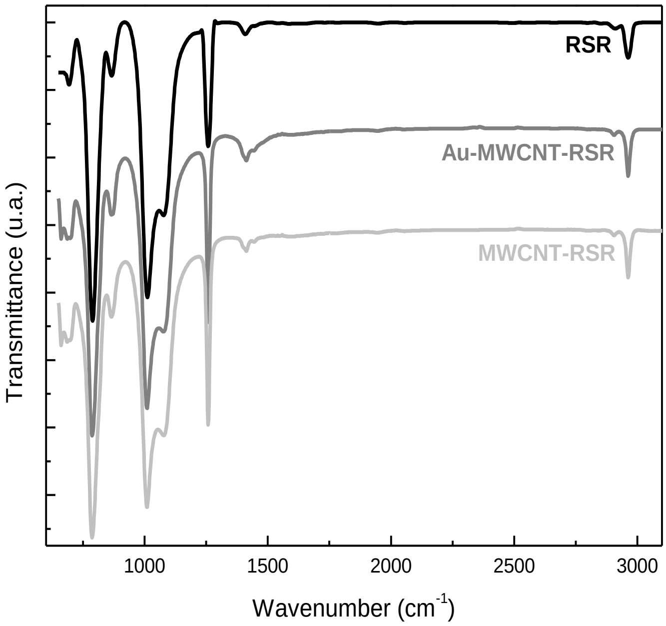

Fig. 2 – ATR-FTIR spectra of RSR and 2.5 wt. % MWCNT-RSR and Au-MWCNT-RSR composites.

The configuration of chemical bonds in the RSR and its composites was analyzed in the 4000–650 cm^{-1} range by Fourier Transform Infrared (FTIR) spectrometry using a Bruker Optics Tensor 27 spectrometer. Measurements of attenuated total internal reflection FTIR (ATR-FTIR) with a ZnSe crystal were performed by averaging 64 scans with a resolution of 4 cm^{-1}. The results, displayed in Fig. 2, show similar spectra in RSR and composites, indicating that no new functional groups could be detected as MWCNTs or Au-MWCNTs are added to the host. The assignment of the FTIR peaks is given in Table 1. The absence of the specific C = C peak around 1600 cm^{-1} in the MWCNT-RSR composites, which would indicate the presence of MWCNTs, is in agreement with other results [14, 15] for pristine nanotubes, supporting the fact that MWCNTs in our samples are of high purity. On the other hand, the similarity of FTIR spectra for MWCNT-RSR and Au-MWCNT-RSR samples suggests insignificant electronic interaction between MWCNTs and Au nanoparticles, observed also in [12].

Table 1

Assignment of IR active functional groups in Fig. 2
(ν–stretching; δ–in-plane bending/scissoring; ρ–in-plane bending/rocking;
as–antisymmetric; s–symmetric)

Wavenumber (cm^{-1})	Assignment
2963	ν (C-H) in CH_3
2906	ν (C-H) in CH_3
1413	δ_{as} (C-H) in Si-CH_3
1258	δ_s (C-H) in Si-CH_3
1078	ν_s (Si-O) in Si-O-Si
1010	ν_{as} (Si-O) in Si-O-Si
865	ρ (C-H) in Si-CH_3
787	ρ (C-H) and ν (Si-C) in Si-CH_3

Thermal analyses of the RSR and its composites containing MWCNTs or Au-MWCNTs were carried out using a Netzsch STA 449C Jupiter in an Al_2O_3 crucible under the flow of 20 mL/min dry air and with a heating speed of 10 K/min. Differential Scanning Calorimetry (DSC) investigations, represented in Fig. 3, indicated a weak endothermic effect in all samples. Thermogravimetry studies (not shown) revealed no visible change in mass for RSR, and MWCNT-RSR and Au-MWCNT-RSR composites, at least up to 150 ^{o}C.

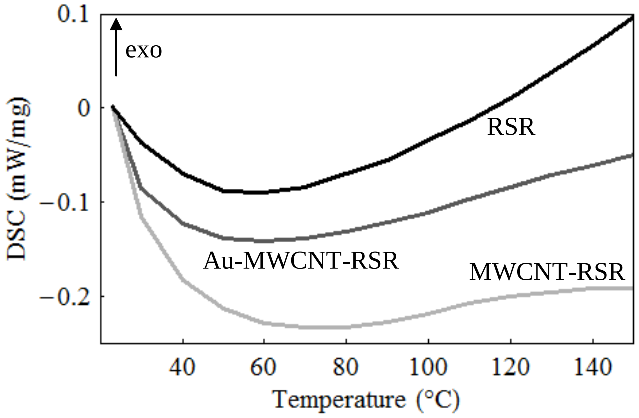

Fig. 3 – Differential Scanning Calorimetry results for the RSR and 2.5 wt. % MWCNT-RSR and Au-MWCNT-RSR composites.

3. DIELECTRIC PROPERTIES OF Au-MWCNT-RSR COMPOSITES

The insulating Au-MWCNT-RSR composite placed between the conducting copper plates, which act as electrical contacts, forms a plane parallel capacitor. The permittivity value of the composite can thus be extracted from the measured capacitance using the classical formula $C = \varepsilon_0 \varepsilon_r S / d$, if the area S and the thickness d of the capacitor are known. The electrical permittivity and dielectric losses of the composite were measured with a Hioki 3532-50 type automatic RLC bridge and a Kethley 2010 multimeter, equipped with a chromel-alumel thermocouple for temperature determinations, the installation being controlled by a computer with GPIB interfaces for automatic data gathering and analysis. The measurements were performed in the frequency interval 300 Hz ÷ 5 MHz and on a wide temperature range, between –50 ^{o}C ÷ +150 ^{o}C, in cooling/heating cycles. All samples were cooled up to –50 ^{o}C starting from room temperature, and then heated up to 150 ^{o}C before being cooled again up to room temperature, with a rate of temperature change in the cycle of about 1.7 ^{o}C/min.

The dependence of dielectric permittivity and losses on temperature, at different frequencies, is shown in Fig. 4a for the RSR and in Figs. 4b–4d for Au-MWCNT-RSR composites with different mass concentrations of Au-MWCNT. In all cases the permittivity decreases at heating for all frequencies and has weak frequency dependence on the whole temperature range. Indeed, ε varies with at most 7 % for the selected frequencies. The decrease of permittivity, as the temperature increases, although not common in polymers, in which the enhanced segmental mobility with temperature leads to an increase of ε at heating, was also observed in nickel-rubber nanocomposites [16], for instance.

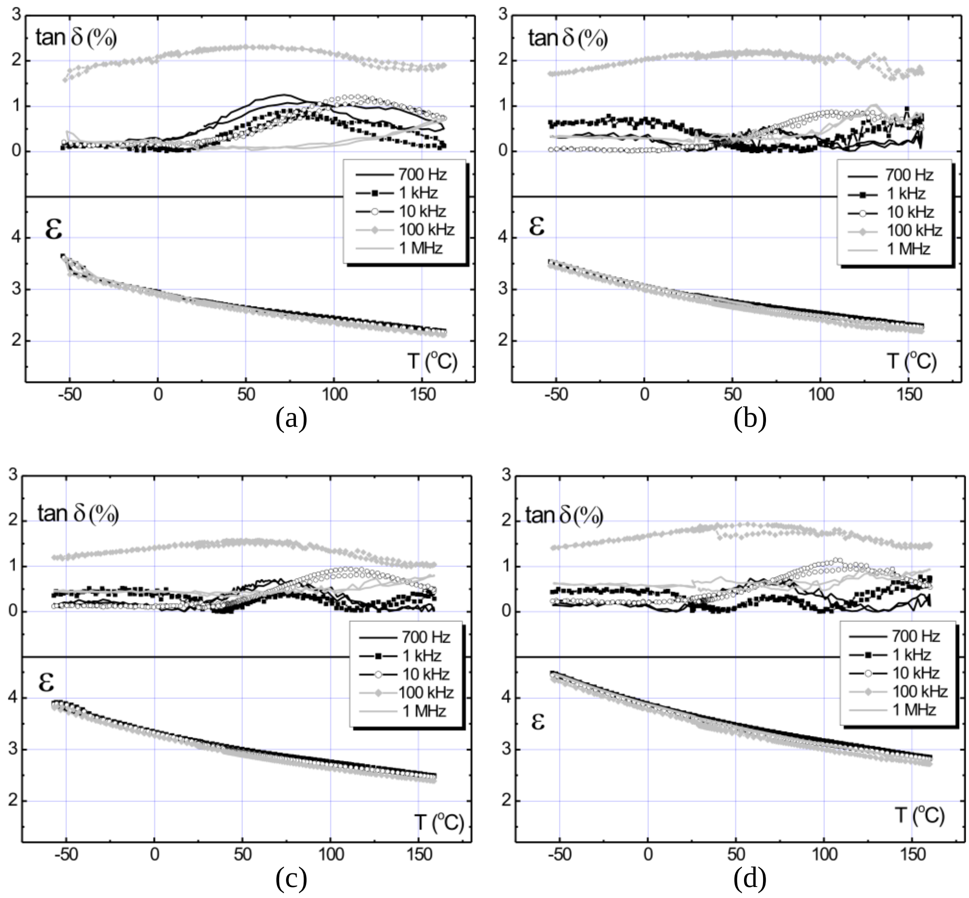

Fig. 4 – Temperature dependence of the permittivity and losses at different frequencies of Au-MWCNT-RSR composites for different Au-MWCNT concentrations: a) 0 wt. %, b) 0.5 wt. %, c) 1.5 wt. %; d) 2.5 wt. %.

The probable cause of this almost linear decrease of the permittivity, as the temperature increases, is the considerable thermal expansion of the RSR, which perturbs the measurement conditions, due to the induced widening of the capacitor [16]. This assumption is supported by the fact that the same behavior is observed also in Au-MWCNT-RSR composites, in which the relative permittivity variation over the whole temperature range, of about 35 %, is similar to that of the RSR, irrespective of the Au-MWCNT mass content. Indeed, the thermal expansion coefficient in CNTs, of 7.5×10^{-6} $^{o}C^{-1}$ [17], is negligible with respect to that in SRs, which has typical values of $2 \div 2.5 \times 10^{-4}$ $^{o}C^{-1}$. The pores in the samples that form during the preparation process could further enhance the thermal expansion of RSR. Also noteworthy is that the permittivity takes reproducible values in cooling-heating cycles, with the exception of temperatures below – 40 ^{o}C. This feature, especially visible in Figs. 4a and 4c, can be attributed to a rapid enhancement of the modulus of rigidity at low temperatures in common silicone rubbers [18].

The dielectric losses in both RSR and Au-MWCNT-RSR composites are small (the highest values are observed at 100 kHz) over the investigated temperature and frequency ranges, consistent with their insulating behavior. Indeed, no conduction could be measured even for the composite with 2.5 wt. % Au-MWCNT, possible due to poor homogeneization of the Au-MWCNT bundles. The small hysteresis in tanδ at heating-cooling cycles, apparent for all samples, indicate the presence of some relaxation mechanism, while the existence of some absorption mechanisms could be inferred from the broad maxima of losses in Figs. 4a–4d. The existence of relaxation phenomena/rearrangements in the polymer matrix is also supported by the weak endothermic effect revealed in DSC analyses in RSR and Au-MWCNT-RSR composites, and shown in Fig. 3.

As evident also from Figs. 4a–4d, the dielectric constants depend on the mass content of Au-MWCNT. This dependence is summarized in Fig. 5, at room temperature. The dielectric permittivity is found to increase as the mass content of Au-MWCNT in the samples, denoted by C, increases. On the other hand, the increase in the mass content of Au-MWCNT does not appear to impose a specific trend on the variation of dielectric losses. Thus, Au-MWCNT-RSR composites can be used as dielectrics with tunable permittivity and low losses over wide temperature ranges. The permittivity enhancement as the mass-content of Au-MWCNT increases is consistent with the Maxwell-Wagner polarization mechanism that predicts interfacial charging in mixtures containing constituents with different electrical permittivities and conductivities, acting as disordered systems. The same polarization mechanism could also explain the frequency and temperature dependences of permittivity, by positioning our frequency investigation range in the high-frequency regime of the composite [19].

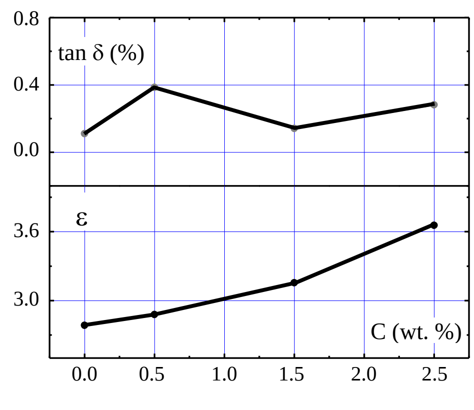

Fig. 5 – Dependence of dielectric parameters on the mass concentration of MWCNTs at 1 kHz and at room temperature.

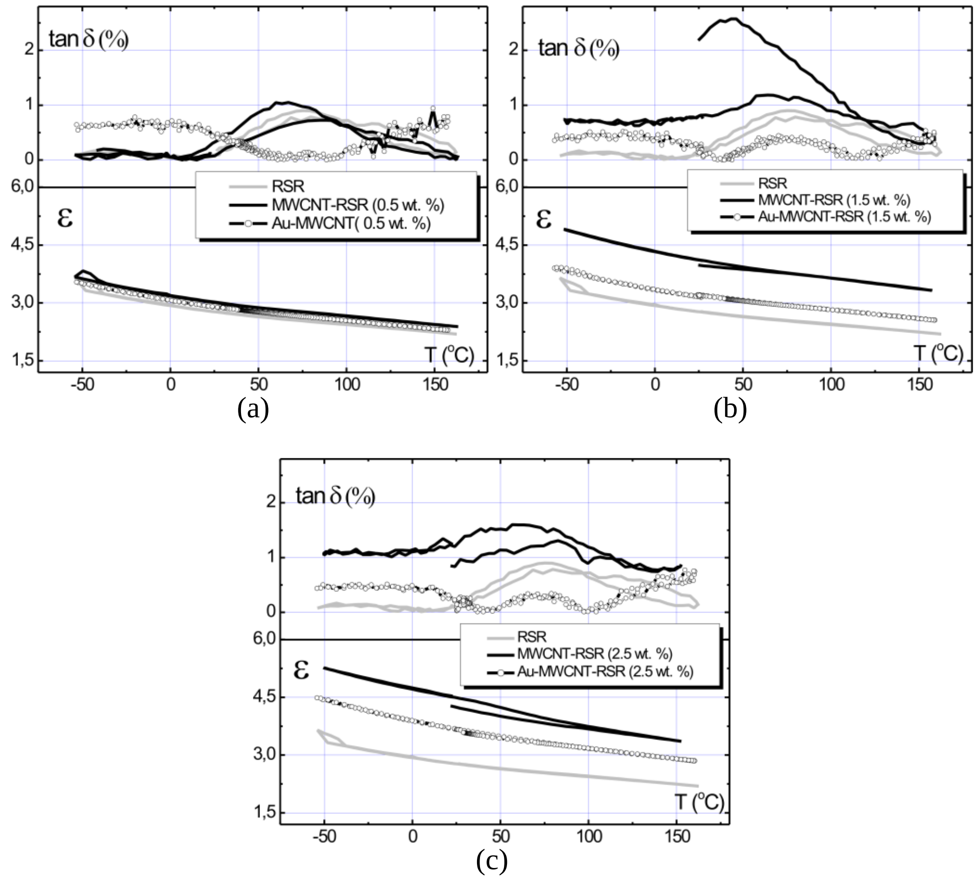

Fig. 6 – Temperature dependence of the permittivity and losses at 1 kHz of RSR, MWCNT-RSR and Au-MWCNT-RSR composites with different Au-MWCNT concentrations:
a) 0.5 wt. %; b) 1.5 wt. %; c) 2.5 wt.%.

It is interesting to compare the seemingly similar temperature dependence of dielectric constants in RSR and Au-MWCNT-RSR composites with the more dissimilar behavior of MWCNT-RSR composites. Such a comparison reveals that (Figs. 6a–6c), whether the permittivity and losses follow almost the same trend in all cases, a significant hysteresis at cooling-heating cycles appear in the dielectric constants of MWCNT-RSR composites. Because spatial re-arrangements of polymeric chains in cooling-heating cycles could take place in all cases, a possible explanation of these results is that the non-reproducibility of dielectric constants in MWCNT-RSR composites is determined mainly by the (partial) damage of the MWCNT due to the large difference in thermal expansion coefficients between MWCNT and the host. The Au nanoparticles could then act as heat sinkers and could ease the thermal stress at the MWCNT-RSR interface and decreases the mechanical stresses in the structures.

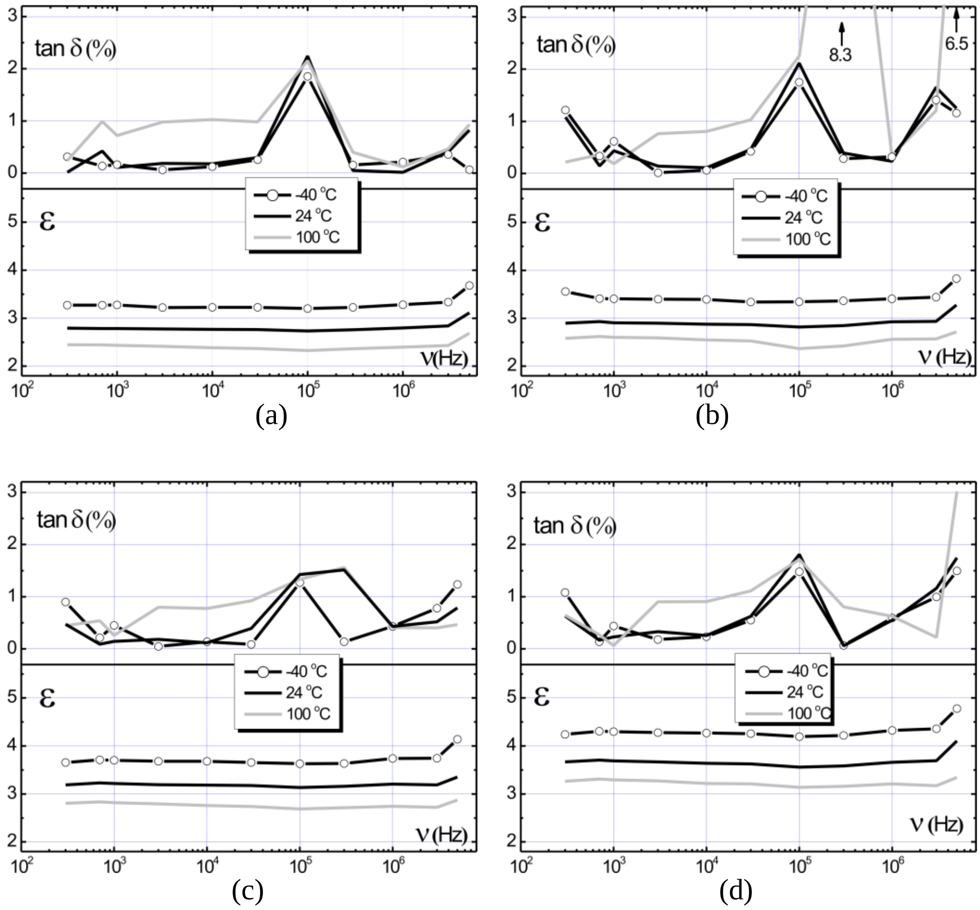

Fig. 7 – Frequency dependence of the permittivity and losses at different temperatures of Au-MWCNT-RSR composites with different Au-MWCNT concentrations: a) 0 wt. %; b) 0.5 wt. %; c) 1.5 wt. %; d) 2.5 wt. %.

The frequency dependence of dielectric permittivity of RSR and its Au-MWCNT composites is also similar, as can be observed from Figs. 7a–7d. In all cases the permittivity varies only slightly with the frequency, except for a slow increase at the high-frequency end of the investigation interval. The losses are relative small values and have a maximum around 100 kHz and increase towards the high-frequency end of the measuring range in all samples, with an additional peak at higher frequencies for the composites with 1.5 wt. % and 2.5 wt. % Au-MWCNT. Similar behaviors of the dielectric constants in SR were attributed to some relaxation phenomena [2].

4. CONCLUSIONS

Composites containing RSR and different mass concentrations of MWCNTs decorated with gold nanoparticles were prepared. Structural characterizations of these composites revealed a low chemical reactivity between the polymer matrix, MWCNTs and Au-decorated MWCNTs. Investigations of the dielectric constant dependence on temperature and frequency over wide ranges show a similar overall behaviour of the RSR and Au-MWCNT-RSR composites. The permittivity can be increased by controlling the mass content of Au-MWCNT, while the losses remain small. The dielectric constants of the Au-MWCNT composites are almost hysteresis-free in cooling-heating cycles suggesting a stable structure, which recommend them in the application as dielectric in equipments working in wide-amplitude temperature and frequency cycles.

REFERENCES

1. S. C. Shit, P. Shah, Natl. Acad. Sci. Lett. **36**, 355-365 (2013).
2. L. K. Namitha, J. Chameswary, S. Ananthakumar and M.T. Sebastian, Ceramics International **39**, 7077-7087 (2013).
3. G. Momen, M. Farzaneh, Rev. Adv. Mater. Sci. **27**, 1-13 (2011).
4. R. Saito, G. Dresselhaus and M. S. Dresselhaus, *Physical Properties of Carbon Nanotubes*, Imperial College Press, London, 1998.
5. P.-C. Ma, N. A. Siddiqui, G. Marom and J.-K. Kim, Composites: Part A **41**, 1345-1367 (2010).
6. S. S. Jyothirmayee Aravind, S. Ramaprabhu, Nanoscience Methods **1**, 102-114 (2012).
7. S. Capula Colindres, K. Aguir, F. C. Sodi, L. Villa Vargas, J. A. Moncayo Salazar and V. Garibay Febles, Sensors **14**, 6806-6818 (2014).
8. J.-C. Valmalette, Z. Tan, H. Abe and S. Ohara, Scientific Reports **4**, 5238 (2014).
9. R. Y. Zhang, H. Olin, Int. J. Biomedical Nanoscience and Nanotechnology **2**, 112-135 (2011).
10. K.-Y. Chun, Y. Oh, J. Rho, J.-H. Ahn, Y.-J. Kim, H. R. Choi and S. Baik, Nature Nanotechnology **5**, 853-857 (2010).
11. K.W. Wagner, Ann. Physik **40**, 817-855 (1913).
12. Y. Lin, K. A. Watson, M. J. Fallbach, S. Ghose, J. G. Smith, Jr., D. M. Delozier, W. Cao, R. E. Crooks and J. W. Connell, ACS Nano **3**, 871-884 (2009).
13. J. Vilčáková, R. Moučka, P. Svoboda, M. Ilčíková, N. Kazantseva, M. Hřibová, M. Mičušík and M. Omastová, Molecules **17**, 13157-13174 (2012).
14. V. T. Le, C. L. Ngo, Q. T. Le, T. T. Ngo, D. N. Nguyen and M. T. Vu, Adv. Nat. Sci.: Nanosci. Nanotechnol. **4**, 035017 (2013).
15. Y. Umasankar, B. Unnikrishnan, S.-M. Chen and T.-W. Ting, Int. J. Electrochem. Sci. **7**, 484-498 (2012).
16. E. Muhammad Abdul Jamal, P. A. Joy, P. Kurian and M. R. Anantharaman, Materials Science and Engineering **B 156**, 24-31 (2009).
17. Y. Maniwa, R. Fujiwara, H. Kira, H. Tou, H. Kataura, S. Suzuki, Y. Achiba, E. Nishibori, M. Takata, M. Sakata, A. Fujiwara and H. Suematsu, Phys. Rev. **B 64**, 241402 (2001).
18. web page: http://www.silicone.jp/e/catalog/pdf/rubber_e.pdf.
19. Y. Chen, D. Or, Water Resources Res. **42**, WO6424 (2006).